Supporting Information.

Nanoscale Patterns on Polar Oxide Surfaces

Mikołaj Lewandowski[1,2], Irene M.N. Groot[1†], Zhi-Hui Qin, [1 ‡], Tomasz Ossowski[3], Tomasz Pabisiak[3], Adam Kiejna[3], Anastassia Pavlovska[4], Shamil Shaikhutdinov1, Hans-Joachim Freund[1] and Ernst Bauer[4,]*

[1] Department of Chemical Physics, Fritz Haber Institute of the Max Planck Society, 14195 Berlin, Germany, [2]NanoBioMedical Centre, Adam Mickiewicz University, 61-614 Poznań, Poland, [3]Institute of Experimental Physics, University of Wrocław, 50-204 Wrocław, Poland, [4]Department of Physics, Arizona State University, Tempe, AZ 85287, USA

Table S1: Work functions of relaxed and unrelaxed (in brackets) terminations of α-Fe_2O_3(0001), compared with other calculations. PBE+4.0 denotes PBE+U with U = 4.0 eV. U^{d}_{ss} denotes surface specific value of U^{d} with the U^{d}, and U^{p} values for oxygen p states, taken from Huang X., *et al*., J. Phys. Chem. C **2016**, *120*, 4919.

Exchange-correlation	Work function (eV)	
	This work	Other calculations
Fe1-termination (Fe-O3-Fe-)		

PW91			4.16 [1]	4.26 [2]			4.3 (3.1) [5]
PBE	4.15	(3.31)					4.0 [6]
PW91+4.0			4.67 [1]	4.77 [2]	4.73 [3]		
PBE+4.0	4.69	(2.79)				4.35 [4]	
PBE+3.81	4.61	(2.78)					
PBE+3.81+U^{p}5.9	4.65	(2.90)					
PBE+U^{d}_{ss}	4.76	(2.73)					
PBE+U^{d}_{ss}+U^{p}5.9	4.68	(2.84)					
Fe2-termination (Fe-Fe-O3-)							
PW91			3.77 [1]				
PBE	3.63	(4.09)					
PW91+4.0			3.17 [1]		2.90 [3]		
PBE+3.81	2.88	(3.85)					
PBE+3.81+U^{p}5.9	2.88	(3.86)					
PBE+U^{d}_{ss}	2.85	(3.92)					
PBE+U^{d}_{ss}+U^{p}5.9	2.85	(3.89)					
O_3-termination (O3- Fe-Fe-)							
PW91			7.53 [1]	7.63 [2]			7.6 (8.3) [5]
PBE	7.44	(8.31)					7.6 [6]
PW91+4.0			8.51 [1]	8.58 [2]	8.52 [3]		
PBE+4.0	8.40	(8.82)				8.40 [4]	
PBE+3.81	8.39	(8.82)					
PBE+3.81+U^{p}5.9	7.60	(7.96)					
PBE+U^{d}_{ss}	8.71	(8.81)					
PBE+U^{d}_{ss}+U^{p}5.9	8.20	(8.00)					
O_1-termination (O1- Fe-Fe-)							

PBE	5.91	(5.71)					
PBE+4.00	6.16	(6.29)					
PBE+3.81	6.19	(6.31)					
PBE+3.81+U^{p}5.9	6.20	(4.85)					
PBE+U^{d}_{ss}	6.27	(6.32)					
PBE+U^{d}_{ss}+U^{p}5.9	5.35	(4.87)					

Table S2. Work functions of relaxed and unrelaxed (in brackets) of magnetite (111) surfaces calculated with PW91+U, effective U =3.61 eV, compared with other calculations.

Termination	Work function (eV)					
	This work		Ref. [7]	Ref. [3]	Ref. [8]	Ref. [9]
Fe_{tet1}	5.49	(3.20)	5.48	5.70	5.76	5.60
O1	7.91	(9.15)	8.09		7.94	
Fe_{oct1} (Kagome)	4.06	(4.12)			3.91	
O2	7.54	(8.80)	7.66	8.03		
Fe_{tet2}	4.20	(4.01)				
Fe_{oct2}	3.00	(4.02)	3.90*		3.15	
Kagome+Fe	4.48	(4.74)				
Ferryl	7.63				7.61	

* The large difference occurs because of different final magnetic configuration which was not considered in previous calculations of the work function. The current result is for the magnetic configuration energetically most favored. Calculations for a magnetic configuration similar to that in the previous work (Ref. [7]) result in a work function of about 3.74 eV.

References

[1]. A. Kiejna *et al*., J. Phys. Condens. Matter, **2012**, *24*, 095003. (E_{cut} = 450 eV.)

[2]. A. Kiejna, T. Pabisiak, J. Phys. Chem. C **2013**, *117*, 24339. (E_{cut} = 450 eV.)

[3]. T. Pabisiak, A. Kiejna, J. Chem. Phys. **2014**, *141*, 134707. (U = 4.0 eV, E_{cut} = 500 eV.)

[4]. T. Pabisiak *et al*., J. Chem. Phys. **2016**, *144*, 044704. (2×2 unit cell, E_{cut} = 500 eV.)

[5]. X-G. Wang *et al*., Phys. Rev. Lett. **1998**, *81*, 1038. (FLAPW)

[6]. J. Jin *et al.*, Surf. Sci. **2007**, *601*, 3082. (E_{cut} = 400 eV.)

[7]. A. Kiejna *et al.*, Phys. Rev. B **2012**, *85*, 125414. (E_{cut} = 500 eV.)

[8]. J. Noh *et al.*, Chem. Mater. **2015**, *27*, 5856. (GGA-PBE, U = 4.0 eV, E_{cut} = 500 eV.)

[9]. T. Pabisiak *et al*., Phys.Chem.Chem.Phys., **2016**, *18*, 18169. (GGA-PBE, U = 4.0 eV, 2×2 unit cell, E_{cut} = 500 eV.)

Table S3. Preparation methods of the α-Fe_2O_3(0001) (a) and Fe_3O_4(111) (b) multilayers. Fe monolayers in Pt(111) atomic density units.

Parameter	Oxide film preparation											
	Hematite						Magnetite					
Cycle #	1	2	3	4	5	6	1	2	3	4	5	6
Fe MLs	1	8	8	8	8	-	1	8	8	8	8	-
P_{O2} [10^{-6} mbar]	10	10	10	10	50	UHV	1	1	1	1	1	UHV
Temperature [K]	1000	900	1000	1000	1100	1100	1000	880	880	880	1000	900
Time [min]	2	5	5	5	10	10	2	5	5	5	10	Flash

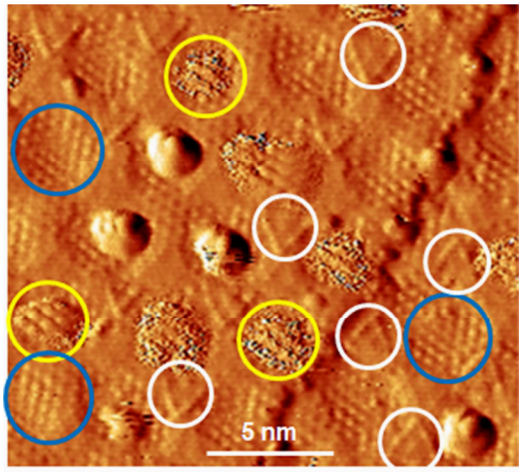

Figure S1. Enlarged section of Fig.7 showing the details in the current image. The color code of the circles is the same as in Fig.7. The noisy γ regions are also covered by an Au adsorption layer but the atoms are dragged along by the high local tunneling current. Most diffuse γ regions in Fig. 7a look this way. Note the opposite orientation of the triangles on the α regions in the neighboring terraces separated by a one monolayer high step, reflecting the different Fe locations in the unit cells in these layers. Bias +1.4 V, current 0.7 nA, PtIr tip.

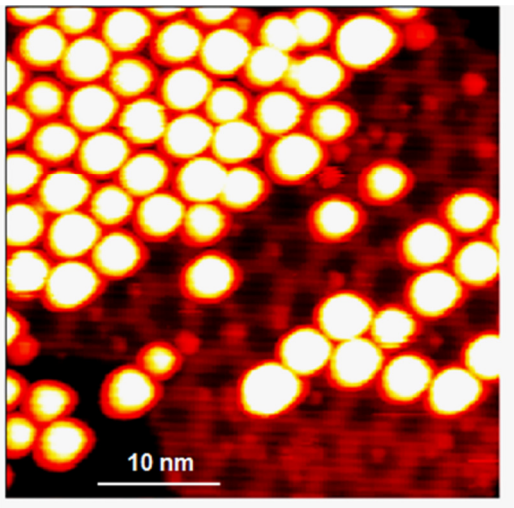

Figure S2. STM image of a region of the thick Au layer on the α-Fe_2O_3(0001) surface shown in Fig. 8, in which part of the Au nanocrystals were removed by the STM tip, illustrating that they are located in the γ regions. Bias +2.0 V, current 0.7 nA, PtIr tip.

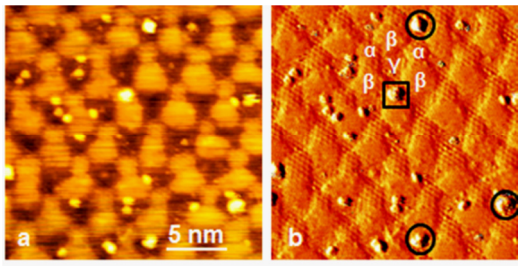

Figure S3. STM topography (a) and current (b) image of a low coverage of Fe on the α-Fe_2O_3(0001) surface. (b) shows the location of the Fe particles with respect to the three surface terminations. The square indicates a particle on the α region, the circles in the γ regions. Bias +2.0 V, current 2.0 nA, PtIr tip.

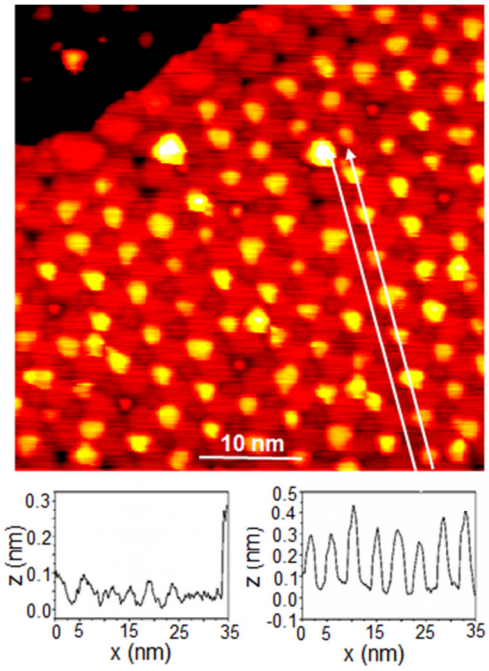

Figure S4. High magnification STM topography image of a high coverage Fe layer on the α-Fe_2O_3(0001) surface showing the location of the Fe nanocrystals with respect to the γ regions and height profiles along the lines in the image, indicating monolayer and double layer nanocrystals. Bias +2.0 V, current 2.0 nA, PtIr tip.

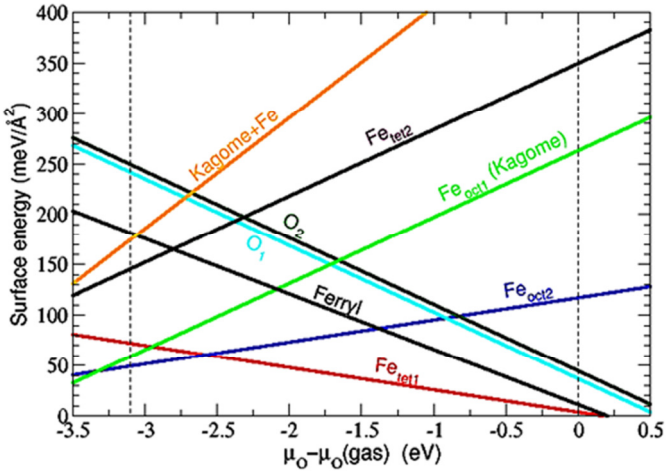

Figure S5. Surface energy of magnetite (111) surface terminations as a function of oxygen chemical potential. The same parameters were used as in table 2.

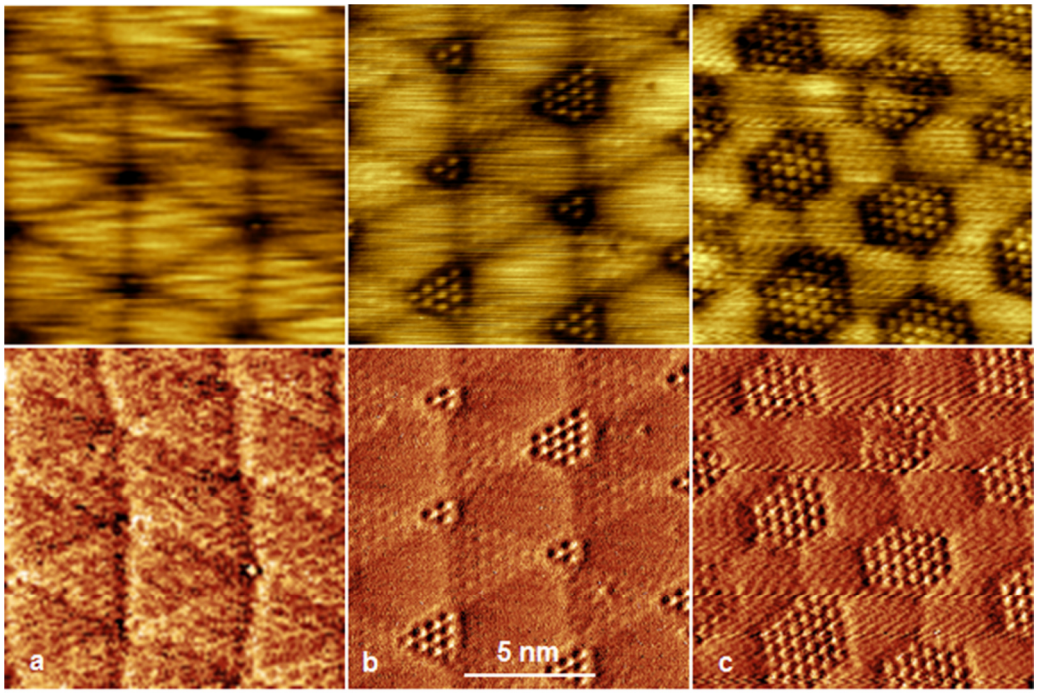

Figure S6. STM topography (top) and current (bottom) images of $Fe_3O_4(111)$ surfaces prepared under different conditions, showing the range of unit cell compositions. Bias +1.0 V, current 1.0 nA (a), +1.4 V, 1.0 nA (b) and +0.25 V, 0.7 nA (c). All images were taken using a PtIr tip.

S7. Comments on the α-$Fe_2O_3(0001)$ surface.

At high O_2 chemical potential μ_{O2} theory predicts oxygen termination, which has also been frequently observed. Because of kinetic limitations high temperatures are needed to facilitate the transition from the superstructure pattern to the (1×1) structure, which requires high oxygen pressures to achieve high μ_{O2} values. In the present study oxidation in about 1 mbar O_2 produced a (1×1) LEED pattern, whose background decreased with increasing temperature up to 800 K. However, wall reactions always caused contamination with Mo. Exposure to about 1 mbar H_2O at 300 K also produced a (1×1) LEED pattern but with strong background and the conversion to

the superstructure pattern begins already upon heating to 600 K in UHV. The TPD spectra (Fig. S7a) of a H_2O-exposed surface shows not only H_2O-related desorption peaks but also CO_2 and CO peaks, suggesting that the (1×1) pattern is stabilized by adsorption of CO- and OH-containing molecules, such as formate. The (1×1) structure could be stabilized by oxidation in $5x10^{-5}$ mbar O_2 of an H_2O-exposed surface up to about 800 K (Fig. S7b). Conversion to the superstructure pattern required heating to ≥ 900 K. A STM topography image of such a (1×1) structure is shown in Fig. S7c (+0.7 V, 0.7 nA, PtIr tip). It has vacancies and unidentified adsorbates, frequently with triangular shape, which can be seen also in the images by other authors[10,11] and have been attributed to adsorbed Fe.[12]

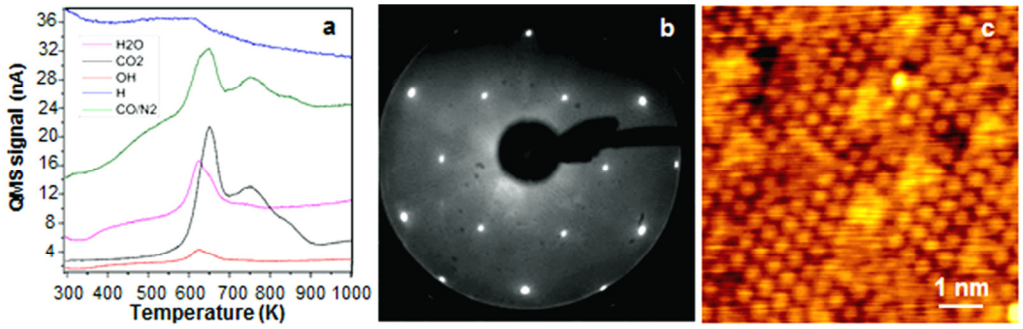

Figure S7. TPD spectra (a), LEED pattern (b) and STM image of a α-Fe_2O_3(0001)-(1×1) surface. For explanation see text. Desorption of the adsorption layer reproduces the superstructure of the clean surface observed before exposure.

References

[10]. Wang, X. G., Weiss, W., Shaikhutdinov, S. K., Ritter, M., Petersen, M., Wagner, F., Schlögl, R. and Scheffler, M. The Hematite (α-Fe_2O_3) (0001) Surface: Evidence for Domains of Distinct Chemistry, *Phys. Rev. Lett.* **1998**, *81*, 1038.

[11]. Shaikhutdinov, S.K. and Weiss, W. Oxygen Pressure Dependence of the α-Fe_2O_3(0001)

Surface Structure, *Surf. Sci. Lett.* **1999**, *432*, L627-L634.

[12]. Eggleston, C. M., Stack, A. G., Rosso, K. M. and Bice, A.M. Atomic Fe(III) on the Hematite Surface: Observation of a Key Reactive Surface Species, *Geochem. Trans.* **2004**, *5,* 33-40.